# Time-Domain Reflectometry Using Arbitrary Incident Waveforms

Te-Wen Pan, Ching-Wen Hsue, *Senior Member, IEEE*, and Jhin-Fang Huang

***Abstract*—A novel time-domain reflectometry technique is developed for detecting the physical structures of transmission lines by using arbitrary waveforms. By discretizing both incident and reflected waves, we formulate the reflection coefficient of a nonuniform transmission line as a polynomial ratio in the $Z$-transform, wherein the numerator and denominator represent the reflected and incident waves, respectively. A reconstruction scheme is derived to obtain the characteristic impedance profile of a transmission line. Some examples are presented to illustrate the validity of this new technique.**

***Index Terms*—Inverse scattering, nonuniform line, time-domain reflectometry (TDR).**

## I. Introduction

THE time-domain reflectometry (TDR) technique has been widely used to characterize the transmission paths in both microwave and optical frequency bands [1]–[6]. Not only does the TDR technique detect the occurrence of discontinuities in transmission lines, it can also measure the impedance variations of discontinuities. The theory of TDR is based on the fact that an incident wave will experience reflection when it encounters a discontinuity. By measuring the reflected wave, we can then evaluate the propagation characteristics of a transmission path.

Most of TDR applications thus far have been limited to the detection of discrete discontinuities of a transmission line. In particular, the conventional TDR technique uses a step wave as an incident source signal. For such a circumstance, each step change in the reflected wave is caused by a discrete isolated discontinuity. However, the reflected wave at a certain time is due to the superposition of all multiple reflected signals that arrive at the input terminal at that instant. Therefore, the conventional TDR technique fails to characterize accurately the discontinuities of a signal line when the transmission line consists of continuously varying or multiple/complex discontinuities. In other words, if the reflected wave at certain time is composed of signal components due to several individual discontinuities, the conventional TDR technique is unable to separate the reflected signal components caused by the corresponding discontinuities. In order to characterize the nonuniform line using the TDR technique, it is pertinent to study thoroughly the internal multiple reflection processes of a transmission line [3], [7].

Manuscript received July 17, 2001; revised January 10, 2002. This work was supported by the National Science Council, R.O.C., under Grant NSC89-2213-EOI1-137.

T.-W. Pan was with the Department of Electronic Engineering, National Taiwan University of Science and Technology, Taipei, Taiwan, R.O.C. He is now with the Gincom Technology Corporation, Taoyuan, Taiwan, R.O.C.

C.-W. Hsue and J.-F. Huang are with the Department of Electronic Engineering, National Taiwan University of Science and Technology, Taipei, Taiwan, R.O.C. (e-mail: cwh@et.ntust.edu.tw).

Digital Object Identifier 10.1109/TMTT.2002.804644

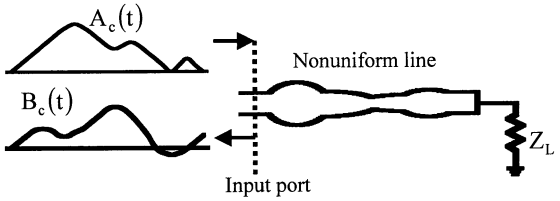


Fig. 1. Nonuniform transmission line and incident/reflected waves.

The wave interactions with nonuniform transmission lines have been studied by many authors for decades [1]–[9]. Most of the studies focused on the direct scattering problems. Some papers [5], [7] were concerned with inverse scattering problems in which the physical parameters of transmission lines were obtained from given scattering parameters at external ports. In this paper, we employ the sampling technique and $Z$-transform method to formulate both incident and reflected waves. As a result, the reflection coefficient of a transmission line can be expressed as a polynomial ratio in the $Z$ domain where the numerator and denominator of the reflection coefficient represent the reflected and incident waves, respectively. We can then arbitrarily select the incident waveform by merely changing the coefficients of the denominator polynominal of the reflection coefficient. For a given nonuniform line, each arbitrary incident wave will generate a distinctive reflected wave. By examining the internal reflection–transmission process of a transmission line, we derive a reconstruction scheme to obtain the characteristic impedance profile of a nonuniform signal line. Several examples are presented to illustrate the validity of this novel TDR technique. It is pertinent to point out the reconstruction scheme presented here is only valid for a nonuniform line that can be approximated by a cascade of ideal transmission lines. The ideal transmission lines have characteristic impedances that are both real and frequency independent.

## II. Theory

Fig. 1 shows a nonuniform transmission line terminated with a load $Z_L$. A wave $A_c(t)$ is incident upon the nonuniform line from the left-hand side, where $t$ is the time. The incident wave can have arbitrary waveshape. This incident wave generates a reflected wave $B_c(t)$ at the input port of the line. If we discretize both the incident and reflected waves, as shown in Fig. 2, we obtain

$$A_c(t) \approx \sum_{n=0}^{N} A_c(t)\delta(t - nT) = A_d[n] \tag{1}$$

and

$$B_c(t) \approx \sum_{n=0}^{N} B_c(t)\delta(t - nT) = B_d[n] \tag{2}$$

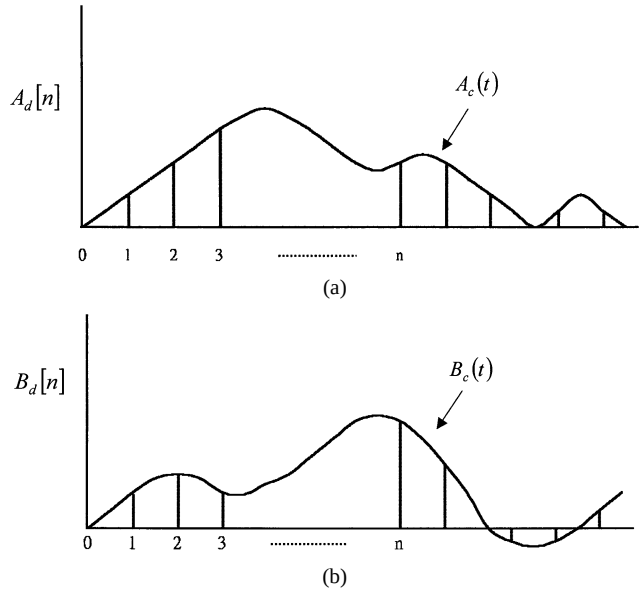


Fig. 2. Discretization of both: (a) incident and (b) reflected waves.

where $n = 1, 2, \ldots, N$, $N$ is the number of samplings, $T$ is the sampling time interval, and $\delta(t)$ is

$$\delta(t) = \begin{cases} 1, & t = 0 \\ 0, & \text{otherwise.} \end{cases}$$

Apparently, $A_d[n]$ and $B_d[n]$ are the sampling values of incident and reflected waves, respectively. The $Z$-transforms of delta sequences $A_d[n]$ and $B_d[n]$ are

$$A_z(z) = \sum_{n=0}^{N} a_n z^{-n} \tag{3}$$

and

$$B_z(z) = \sum_{n=0}^{N} b_n z^{-n} \tag{4}$$

respectively, where $a_n = A_d[n]$, $b_n = B_d[n]$, and $z = e^{j\omega T}$, where $\omega$ is the angular frequency. We now define a function $D_z(z)$ as the ratio of $B_z(z)$ to $A_z(z)$, i.e.,

$$D_z(z) = \frac{\sum_{n=0}^{N} b_n z^{-n}}{\sum_{n=0}^{N} a_n z^{-n}}. \tag{5}$$

Note that $D_z(z)$ may be viewed as the reflection coefficient of the transmission line in the $Z$ domain. In other words, $D_z(z)$ is the system function of the transmission line in the consideration of reflection of transmission line. If we set $z = e^{j\omega T}$ in (5), we obtain the reflection coefficient in the frequency domain. The form in (5) is the same as that obtained by treating a nonuniform line as a cascade of ideal transmission lines [9]. We furthermore express $D_z(z)$ in terms of impulse response. We then have

$$D_z(z) = \frac{\sum_{n=0}^{N} b_n z^{-n}}{\sum_{n=0}^{N} a_n z^{-n}} = \sum_{n=0}^{\infty} d_n z^{-n}. \tag{6}$$

The delta sequence $d_n$ is the impulse response of the nonuniform transmission line, i.e., $d_n$ is the reflected wave when a unit impulse signal is incident upon the signal line. $d_n (n = 0, 1, 2)$ is related to $a_n$ and $b_n$ in the following ways:

$$d_0 = D_z(z)|_{z^{-1}=0} = \frac{b_0}{a_0} \tag{7a}$$

$$d_1 = \left[D_z(z) - d_0\right] z|_{z^{-1}=0} = \frac{b_1 - d_0 a_1}{a_0} \tag{7b}$$

$$d_2 = \left[D_z(z) - d_0 - d_1 z^{-1}\right] z^2|_{z^{-1}=0} = \frac{b_2 - d_0 a_2 - d_1 a_1}{a_0}. \tag{7c}$$

A close examination on (6) and (7) reveals that $a_n$, $b_n$, and $d_n$ satisfy the following recursion equation:

$$d_n = \begin{cases} \dfrac{b_0}{a_0}, & n = 0 \\ \dfrac{\left(b_n - \sum_{i=0}^{n-1} d_i a_{n-i}\right)}{a_0}, & n = 1, 2, \ldots, N. \end{cases} \tag{8}$$

If all $a_n$ and $b_n$ are given, we then use the above equation to obtain $d_n$.

We know that $d_n$ is the impulse response occurring at the instant $nT$. As a result, $d_n a_o$ is the reflected wave caused by the wavefront $a_o$ of the incident signal. On the other hand, due to the internal multiple reflection processes of a nonuniform line, $b_n$ is the summation of the reflected signal components that arrive at the input end at the instant $nT$. To compare the digital signal-processing (DSP) concepts we have developed thus far with the progressive process of the reflected wave, we show in Fig. 3(a) a multiple-section signal line, where $Z_n (n \leq N)$ is the characteristic impedance, $\tau$ is the propagation delay, and $S_{nn} (n \leq N)$ represents the reflection coefficient at the junction between sections $n$ and $n + 1$. Notice that $\tau$ is equal to $(1/2)T$. The relationship between $d_n$ and $S_{nn}$ can be expressed as follows:

$$d_0 = S_{00} \tag{9a}$$

$$d_1 = (1 + S_{00}) S_{11} (1 - S_{00}) \tag{9b}$$

$$d_2 = (1 + S_{00}) S_{11} (-S_{00}) S_{11} (1 - S_{00}) + (1 + S_{00})(1 + S_{11})(S_{22})(1 - S_{11})(1 - S_{00}). \tag{9c}$$

If all $d_n$ are given, we can get the reflection coefficients $S_{nn}$ by solving (9) sequentially. An examination on the wave progressive behavior in a multisection line may help us obtain the reflection coefficient $S_{nn}$ through (9). As shown in Fig. 3(b), waves suffer from multiple transmissions and reflections at respective junctions. If a unit impulse is incident upon junction 0 between sections 0 and 1 at time $t = 0$, it will generate a reflected wave $d_0$ at $t = 0$. The reflected wave $d_o$ is equal to $S_{00}$. At $t = \tau$, the incident wave reaches junction 1 and it is split into two parts, namely, $w1$ and $w2$. At $t = 2\tau$, wave $w1$ transmits through junction 0 and generates the reflected wave $d_1$, which is equal to $(1 + S_{00}) S_{11} (1 - S_{00})$. Note that $(1 + S_{00})$ is the transmission coefficient at junction 0 from the left- to right-hand side, $S_{11}$ is the reflection coefficient at junction 1 from the left-hand side, and $(1 - S_{00})$ is the transmission coefficient at junction 0 from the right- to left-hand side. If both $S_{00}$

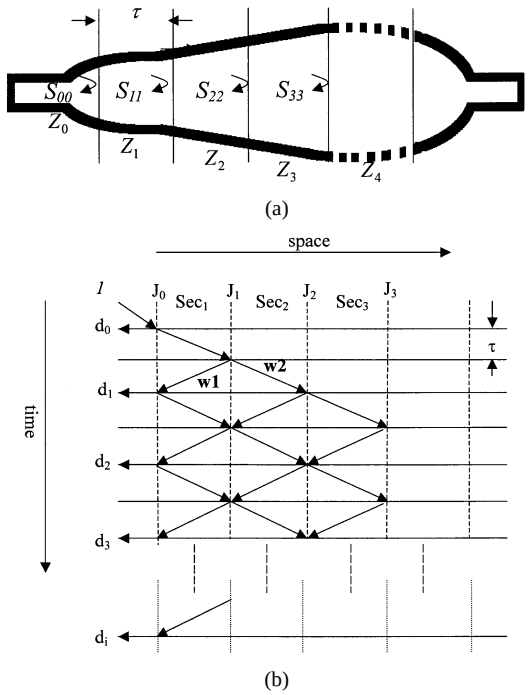


Fig. 3. (a) Nonuniform transmission line is represented by a cascade of ideal transmission lines. (b) The progressive behavior of waves on the signal line.

and $d_1$ are known, $S_{11}$ is then obtained. We may obtain $S_{nn}$ by observing the progressive behavior of waves at junction 0 and all other discontinuity junctions. It is difficult to generalize (9) and obtain $S_{nn}$ analytically. However, because the progressive behavior of waves follows specific rules, we may edit an algorithm and use a computer to solve the problem. Fig. 4 shows the flowchart of the algorithm. It solves $S_{nn}$ when all $d_n$ are given. Notice that sec(n).inc in the flowchart represents the incident wave from the left- to right-hand side on section $n$ and sec(n).ref represents the reflected wave.

The impedance profile of the signal line is related to $S_{nn}$ as follows:

$$Z_{n+1} = Z_n \frac{1+S_{nn}}{1-S_{nn}}. \tag{10}$$

After obtaining the impedance profile, we then get the physical length of each finite line by setting $l_n = \tau v_n$ [11], where $v_n$ is the propagation velocity of the signal in the corresponding line. Note that, for a given characteristic impedance $Z_n$ and dielectric constant $\varepsilon_r$ in a microstrip-line configuration, we obtain the ratio of strip width to substrate thickness [11], which yields the effective dielectric constant of a microstrip line.

## III. Numerical Examples

We present several examples to illustrate the validity of the above theory. We consider a triangular taper that has the profile distribution of characteristic impedance as follows:

$$Z(x) = \begin{cases} Z_0 e^{2(x/L)^2 \ln(Z_L/Z_0)}, & \text{for } 0 \le x \le \dfrac{L}{2} \\ Z_0 e^{((4x/L)-(2x^2/L)-1)^2 \ln(Z_L/Z_0)}, & \text{for } \dfrac{L}{2} \le x \le L \end{cases} \tag{11}$$

where $x$ is the space variable, $L$ is the physical length, and $Z_o$ and $Z_L$ are the characteristic impedances on the incident and transmitted ends of the triangular taper, respectively. When a wave is incident upon the taper, it will produce a reflected wave at the incident port. To characterize the impedance profile of this taper line, as mentioned previously, we may select arbitrary waveforms as the incident signals. Fig. 5 shows three arbitrary signals, namely, two single-sinusoidal waves and a single-triangular (or sawtooth) wave. The single-sinusoidal incident signal is given by

$$V_{\text{int}}(t) = \begin{cases} A_s \sin \omega_0 t, & \text{for } 0 \le \omega_0 t \le 2\pi \\ 0, & \text{elsewhere} \end{cases} \tag{12}$$

where $A_s$ is the amplitude and $\omega_0$ is the angular frequency of the signal. In Fig. 5, the angular frequencies for two sinusoidal signals are $\omega_0 = 2\pi \cdot 10^9$ and $\omega_0 = \pi \cdot 10^9$, respectively. The amplitude $A_s$ is 1 V. These two signal waves extend over 1 and 2 ns, respectively, in the time domain. The triangular signal is, on the other hand, determined by

$$V_{\text{int}}(t) = \begin{cases} A_t \dfrac{t}{t_b}, & \text{for } 0 \le t_b \\ A_t \left(1 - \dfrac{t-t_b}{t_a-t_b}\right), & \text{for } t_b \le t \le t_a \\ 0, & \text{elsewhere} \end{cases} \tag{13}$$

where $A_t$ is the amplitude of the signal, $t_a$ is the duration of triangular wave, and $t_b \le t_a$. For the waveform shown in Fig. 5, we have $t_b = 0.5$ ns and $t_a = 1$ ns. We show in Fig. 6 the reflected waves $V_r(t)$ when the incident waves in Fig. 5 are incident upon the triangular taper in (11), where $Z_0 = 50\ \Omega$, $Z_L = 80\ \Omega$, and $L = 10$ cm. The propagation velocity of signal in the triangular taper is set to $10^{10}$ cm/s. Thus, the propagation delay across the taper line is 1 ns. Therefore, the pulsewidths of three incident signals are either the same as or larger than the propagation delay of signal line. Furthermore, we assume that the propagation delay of the line is independent of characteristic impedance distribution $Z(x)$. Notice that the reflected waves are obtained when the load end is terminated with a matched load. To reconstruct the triangular taper, we first convert both the incident and reflected waves into the $Z$-transform polynomials by employing (1)–(4), i.e., we get the coefficients $a_n$ and $b_n$ that represent the incident and reflected waves, respectively. The reconstructed tapers are then obtained by using recursive equations (8)–(10). As shown in Fig. 7, three numerically reconstructed lines are almost identical with the original triangular taper. Note that the signal line shown in (11) is assumed to be lossless and dispersionless. The results reveal that we may employ arbitrary incident waves to characterize transmission lines. In particular, the pulsewidth has little effect on the space resolution of reconstructed lines. The conventional TDR technique employs a step signal as the incident wave, wherein the rise time of the step signal ranges from several picoseconds to several tens of picoseconds. The requirements of both arbitrary rise time and pulsewidth separate our novel scheme from the conventional TDR technique.

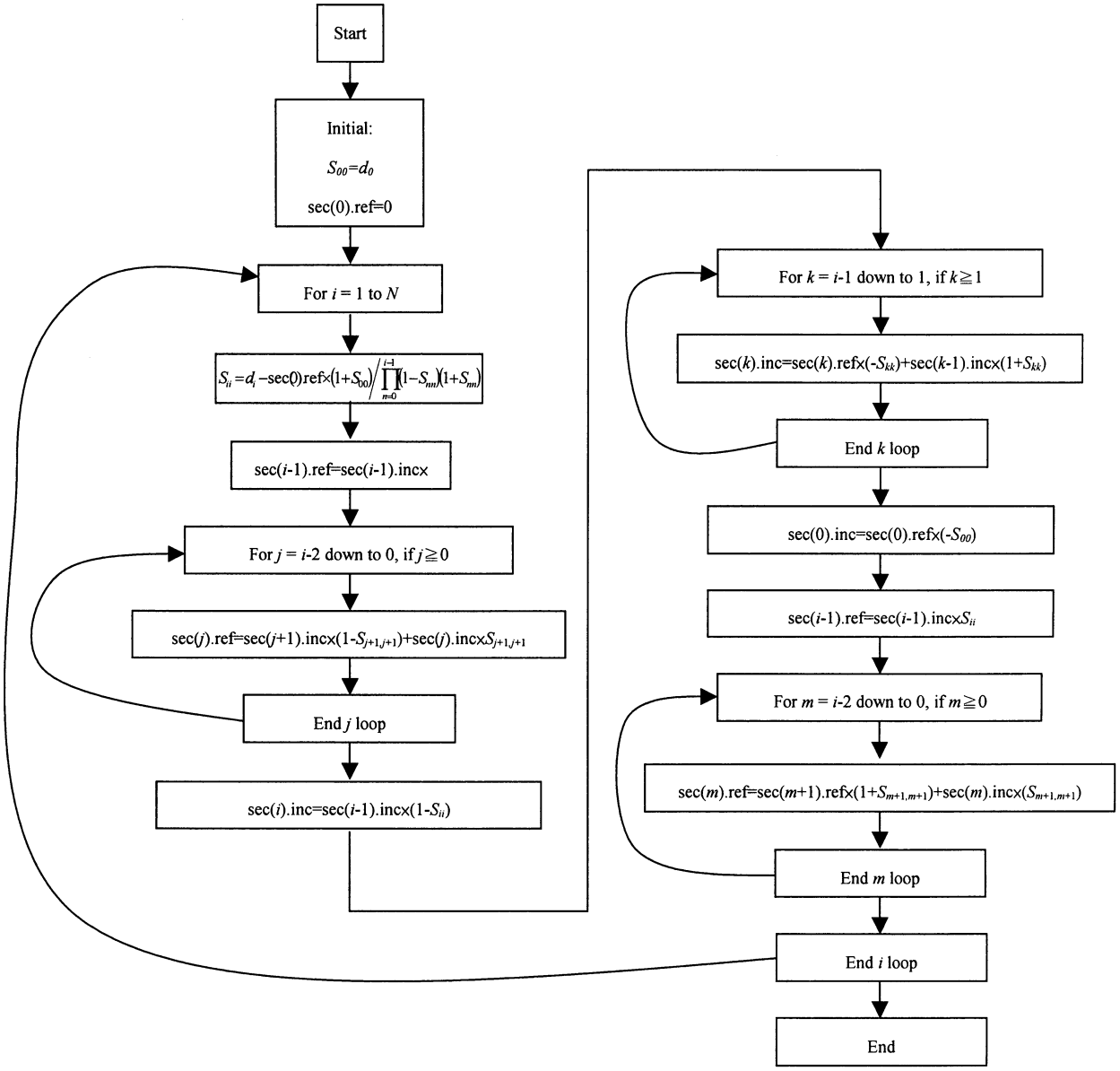


Fig. 4. Flowchart of the algorithm that solves $S_{nn}$ when all $d_n$ are given.

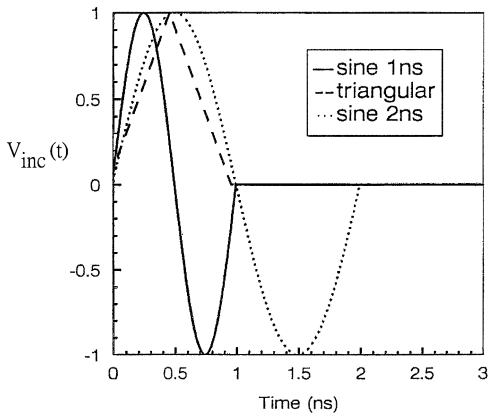


Fig. 5. Three arbitrary incident waves.

## IV. Experimental Results

Fig. 8 shows a layout of a nonuniform microstrip wherein the characteristic impedance distribution of the microstrip is controlled by changing the strip width of the line. The characteristic impedance of the nonuniform line varies between 20–75 Ω and the line is 14-cm long. This microstrip is built on a Duroid substrate having a thickness of 1.52 mm (60 mil) and a dielectric constant of 3.38. Fig. 9 shows the reflected waves $V_r(t)$ when a triangular and two sinusoidal waves in Fig. 5 are incident upon the nonuniform microstrip. We measure the frequency-domain scattering parameter of the nonuniform line by using an HP8510C network analyzer. The multiplication of this scattering parameter with the Fourier transforms of the incident signal yields the reflected signal in the frequency domain. Finally, we obtain the time-domain reflected wave by taking the inverse Fourier transform of the frequency-domain response [10]. Due to the continuous variation of characteristic impedance of the nonuniform microstrip, the reflected waves suffer severe waveform distortion. The transient ripples of the reflected waves due to a triangular incident wave and two sinusoidal waves last longer than the pulse duration of

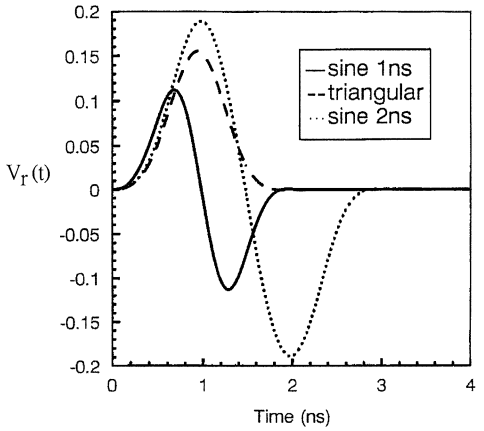


Fig. 6. Reflected waves generated by a triangular taper and the incident waves in Fig. 5.

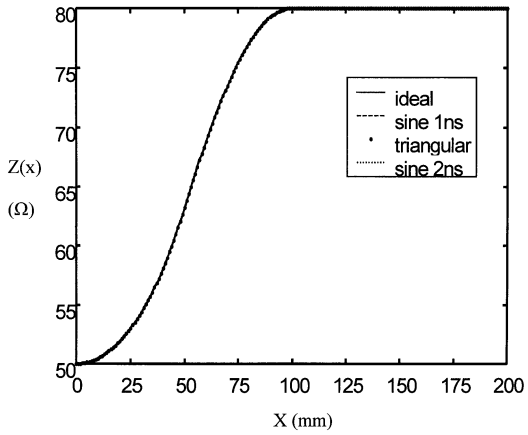


Fig. 7. Reconstructed triangular tapers and the original taper as a function of $x$.

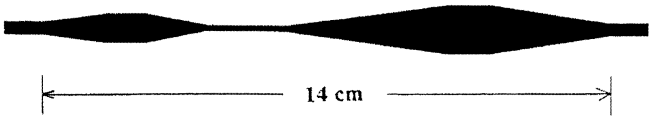


Fig. 8. Physical layout of a nonuniform microstrip.

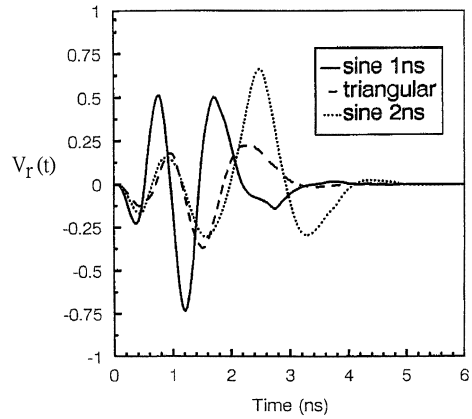


Fig. 9. Reflected waves generated by incident waves and the microstrip in Fig. 8.

respective incident waves. Note that the propagation delay for the signal traveling across the nonuniform microstrip in Fig. 8 is approximately 0.85 ns. For this specific example, the theory

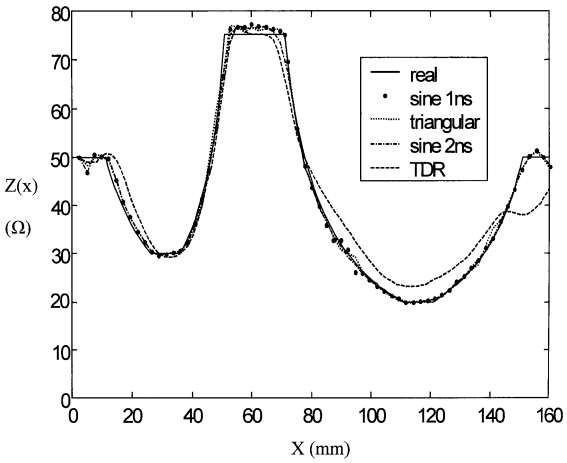


Fig. 10. Characteristic impedance distribution of the reconstructed and original microstrips.

presented in Section II illustrates that the reflected signal lying between 0–1.7 ns is sufficient to determine the characteristic impedance profile of the nonuniform line. However, to assure the completion of reconstruction procedure, the whole transition ripple should be taken into consideration. When the whole transition ripple is considered in the reconstruction process, the reconstructed signal line consists of a nonuniform line and an extra uniform line representing a matched load. Fig. 10 shows the characteristic impedance distribution of three reconstructed lines. To get these three lines, we first divide each of the reflected waves in Fig. 9 into 100 subintervals to get the $b_n$ series, i.e., $T = (6/100)$ ns is used in the numerical evaluation. The impedance profile in the time domain is obtained by using both the reconstruction formulas (8)–(10) and the reconstruction algorithm shown in Fig. 3. We attain the physical length of the reconstructed line by using $l_n = \tau v_n$, where $\tau$ is the propagation delay and $v_n$ is the propagation velocity of signal in the corresponding subsection line. Obviously, three reconstructed lines are in good agreement with the original signal line. To compare our reconstruction scheme with the conventional TDR technique, we also show in Fig. 10 the TDR measurement results. The accuracy of our reconstruction scheme is better than that of the conventional TDR technique.

We usually employ a narrow pulse signal as the incident wave to improve the space resolution of the reconstructed transmission line. However, the above results reveal that signals of any waveshapes or pulsewidths can be used to detect the characteristic impedance profiles of signal lines. This is true because the spatial resolution of the transmission line is a function of the sampling interval rather than the duration of the incident pulse. Although the envelopes of the incident waves in the space domain are larger than the physical length of a nonuniform line, the new TDR technique can still differentiate the details of a signal line. Such a property is based on the fact that this novel scheme embraces internal multiple transmission-reflection processes of a nonuniform signal line. As a result, a slow slew-rate incident wave will not degrade the resolution of a reconstructed transmission line. One should note that a very slow slew-rate incident wave may cause greater computation errors in $a_n$, $b_n$, and $d_n$, which will reduce the accuracy of the reconstructed result.

## V. Conclusion

We have developed a novel technique to reconstruct a nonuniform transmission line by using arbitrary incident waveforms. For practical applications, arbitrary waveforms are easier to obtain in many electronic circuits. In particular, the resolution of such a reconstruction technique could exceed that of the conventional TDR technique, which employs a step signal or narrow pulse as the incident wave.

## References


[1] W. R. Scott and G. S. Smith, "Error corrections for an automated time-domain network analyzer," *IEEE Trans. Instrum. Meas.*, vol. IM-35, pp. 300–303, Sept. 1986.

[2] N. S. Nahman, "Picosecond-domain waveform measurement: Status and future directions," *IEEE Trans. Instrum. Meas.*, vol. IM-32, pp. 117–124, Mar. 1983.

[3] T. Dhaene, L. Martens, and D. D. Zutter, "Calibration and normalization of time domain network analyzer measurements," *IEEE Trans. Microwave Theory Tech.*, vol. 42, pp. 580–589, Apr. 1994.

[4] P. I. Somlo and D. L. Hollway, "Microwave locating reflectometer," *Electron. Lett.*, vol. 5, pp. 468–469, Oct. 1969.

[5] D. L. Philen, I. A. White, J. F. Kuhl, and S. C. Mettler, "Single-mode fiber TDR: Experiment and theory," *IEEE Trans. Microwave Theory Tech.*, vol. MTT-30, pp. 1487–1496, Oct. 1982.

[6] K. Aoyama, K. Nakazama, and T. Itoh, "Optical time-domain reflectometry in a single-mode fiber," *IEEE J. Quantum Electron.*, vol. QE-17, pp. 862–868, June 1981.

[7] P. P. Roberts and G. E. Town, "Design of microwave filters by inverse scattering," *IEEE Trans. Microwave Theory Tech.*, vol. 43, pp. 739–743, Apr. 1995.

[8] V. P. Meschanov, I. A. Rasukova, and V. D. Tupikin, "Stepped transformers on TEM-transmission lines," *IEEE Trans. Microwave Theory Tech.*, vol. 44, pp. 793–798, June 1996.

[9] T.-W. Pan and C.-W. Hsue, "Modified transmission and reflection coefficients of nonuniform transmission lines and their applications," *IEEE Trans. Microwave Theory Tech.*, vol. 46, pp. 2092–2097, Dec. 1998.

[10] A. V. Oppenheim and R. W. Shafer, *Discrete-Time Signal Processing*. New Jersey: Prentice-Hall, 1989.

[11] D. M. Pozar, *Microwave Engineering*. Reading, MA: Addison-Wesley, 1990.


**Te-Wen Pan** was born on August 28, 1969, in Taipei, Taiwan, R.O.C. He received the B.S., M.S., and Ph.D. degrees in electronic engineering from the National Taiwan University of Science and Technology, Taipei, Taiwan, R.O.C., in 1994, 1996, and 2000, respectively.

From 1996 to 1997, he was with Electronic Testing Center, Taoyuan, Taiwan, R.O.C., where he was involved with electromagnetic compatibility testing, and research. From 2000 to 2002, he was a Researcher with the Benq Corporation (formerly Acer Communication and Multimedia Inc.). Since March 2002, he has been the Research and Development Group Leader with the Gincom Technology Corporation, Taoyuan, Taiwan, R.O.C., which is a newly founded company devoting to low-temperature co-fired ceramic (LTCC) modules, RF components design, and wireless communication system integration. His current research interests are electromagnetic compatibility, microwave circuit design, electromagnetic compatibility, and RF system integration.

**Ching-Wen Hsue** (S'85–M'85–SM'91) was born in Tainan, Taiwan, R.O.C. He received the B.S. and M.S. degrees in electrophysics and electronics from the National Chiao-Tung University, Hsin-Chu, Taiwan, R.O.C., in 1973 and 1975, respectively, and the Ph.D. degree from the Polytechnic University of New York, Brooklyn, NY, in 1985.

From 1975 to 1980, he was a Research Engineer with the Telecommunication Laboratories, Ministry of Communications, Taiwan, R.O.C. From 1985 to 1993, he was a Member of Technical Staff with Bell Laboratories, Princeton. NJ. In 1993, he joined the Department of Electronic Engineering, National Taiwan University of Science and Technology, Taipei, Taiwan, R.O.C., as a Professor, and from August 1997 to July 1999, he was the Department Chairman. His current interests are in pulse-signal propagation in lossless and lossy transmission media, electromagnetic inverse scattering, applications of discrete-time techniques to microwave circuits, and electromagnetic compatibility.

**Jhin-Fang Huang** was born in Taiwan, R.O.C., in 1950. He received the B.S. and M.S. degrees in electrical engineering from the National Cheng-Kung University, Tainan, Taiwan, R.O.C., in 1973 and 1975, respectively, and the Ph.D. degree in electrical and computer engineering from the University of Kansas, Lawrence, in 1989.

In 1989, he joined the Electronic Engineering Department, National Taiwan University of Science and Technology, Taiwan, R.O.C., as an Associate Professor, where he is currently engaged in research in microwave circuits and cable TV broadcast networks.

Dr. Huang is a member of the Institute of Satellite and Cable TV Technology and was its the chairman from 1997 to 2000.